

Observation of $D^0 \rightarrow K_1(1270)^- e^+ \nu_e$

M. Ablikim¹, M. N. Achasov^{10,c}, P. Adlarson⁶⁷, S. Ahmed¹⁵, M. Albrecht⁴, R. Aliberti²⁸, A. Amoroso^{66A,66C}, M. R. An³², Q. An^{63,49}, X. H. Bai⁵⁷, Y. Bai⁴⁸, O. Bakina²⁹, R. Baldini Ferrolli^{23A}, I. Balossino^{24A}, Y. Ban^{38,k}, K. Begzsuren²⁶, N. Berger²⁸, M. Bertani^{23A}, D. Bettoni^{24A}, F. Bianchi^{66A,66C}, J. Bloms⁶⁰, A. Bortone^{66A,66C}, I. Boyko²⁹, R. A. Briere⁵, H. Cai⁶⁸, X. Cai^{1,49}, A. Calcaterra^{23A}, G. F. Cao^{1,54}, N. Cao^{1,54}, S. A. Cetin^{53A}, J. F. Chang^{1,49}, W. L. Chang^{1,54}, G. Chelkov^{29,b}, D. Y. Chen⁶, G. Chen¹, H. S. Chen^{1,54}, M. L. Chen^{1,49}, S. J. Chen³⁵, X. R. Chen²⁵, Y. B. Chen^{1,49}, Z. J. Chen^{20,l}, W. S. Cheng^{66C}, G. Cibinetto^{24A}, F. Cossio^{66C}, X. F. Cui³⁶, H. L. Dai^{1,49}, X. C. Dai^{1,54}, A. Dbeyssi¹⁵, R. E. de Boer⁴, D. Dedovich²⁹, Z. Y. Deng¹, A. Denig²⁸, I. Denysenko²⁹, M. Destefanis^{66A,66C}, F. De Mori^{66A,66C}, Y. Ding³³, C. Dong³⁶, J. Dong^{1,49}, L. Y. Dong^{1,54}, M. Y. Dong^{1,49,54}, X. Dong⁶⁸, S. X. Du⁷¹, Y. L. Fan⁶⁸, J. Fang^{1,49}, S. S. Fang^{1,54}, Y. Fang¹, R. Farinelli^{24A}, L. Fava^{66B,66C}, F. Feldbauer⁴, G. Felici^{23A}, C. Q. Feng^{63,49}, J. H. Feng⁵⁰, M. Fritsch⁴, C. D. Fu¹, Y. Gao⁶⁴, Y. Gao^{38,k}, Y. Gao^{63,49}, Y. G. Gao⁶, I. Garzia^{24A,24B}, P. T. Ge⁶⁸, C. Geng⁵⁰, E. M. Gersabeck⁵⁸, A. Gilman⁶¹, K. Goetzen¹¹, L. Gong³³, W. X. Gong^{1,49}, W. Gradl²⁸, M. Greco^{66A,66C}, L. M. Gu³⁵, M. H. Gu^{1,49}, S. Gu², Y. T. Gu¹³, C. Y. Guan^{1,54}, A. Q. Guo²², L. B. Guo³⁴, R. P. Guo⁴⁰, Y. P. Guo^{9,h}, A. Guskov²⁹, T. T. Han⁴¹, W. Y. Han³², X. Q. Hao¹⁶, F. A. Harris⁵⁶, N. Hüsken^{22,28}, K. L. He^{1,54}, F. H. Heinsius⁴, C. H. Heinz²⁸, T. Held⁴, Y. K. Heng^{1,49,54}, C. Herold⁵¹, M. Himmelreich^{11,f}, T. Holtmann⁴, Y. R. Hou⁵⁴, Z. L. Hou¹, H. M. Hu^{1,54}, J. F. Hu^{47,m}, T. Hu^{1,49,54}, Y. Hu¹, G. S. Huang^{63,49}, L. Q. Huang⁶⁴, X. T. Huang⁴¹, Y. P. Huang¹, Z. Huang^{38,k}, T. Hussain⁶⁵, W. Ikegami Andersson⁶⁷, W. Imoehl²², M. Irshad^{63,49}, S. Jaeger⁴, S. Janchiv^{26,j}, Q. Ji¹, Q. P. Ji¹⁶, X. B. Ji^{1,54}, X. L. Ji^{1,49}, Y. Y. Ji⁴¹, H. B. Jiang⁴¹, X. S. Jiang^{1,49,54}, J. B. Jiao⁴¹, Z. Jiao¹⁸, S. Jin³⁵, Y. Jin⁵⁷, T. Johansson⁶⁷, N. Kalantar-Nayestanaki⁵⁵, X. S. Kang³³, R. Kappert⁵⁵, M. Kavatsyuk⁵⁵, B. C. Ke^{43,1}, I. K. Keshk⁴, A. Khoukaz⁶⁰, P. Kiese²⁸, R. Kiuchi¹, R. Kliemt¹¹, L. Koch³⁰, O. B. Kolcu^{53A,e}, B. Kopf⁴, M. Kuemmel⁴, M. Kuessner⁴, A. Kupsc⁶⁷, M. G. Kurth^{1,54}, W. Kühn³⁰, J. J. Lane⁵⁸, J. S. Lange³⁰, P. Larin¹⁵, A. Lavania²¹, L. Lavezzi^{66A,66C}, Z. H. Lei^{63,49}, H. Leithoff²⁸, M. Lellmann²⁸, T. Lenz²⁸, C. Li³⁹, C. H. Li³², Cheng Li^{63,49}, D. M. Li⁷¹, F. Li^{1,49}, G. Li¹, H. Li⁴³, H. Li^{63,49}, H. B. Li^{1,54}, H. J. Li¹⁶, J. L. Li⁴¹, J. Q. Li⁴, J. S. Li⁵⁰, Ke Li¹, L. K. Li¹, Lei Li³, P. R. Li³¹, S. Y. Li⁵², W. D. Li^{1,54}, W. G. Li¹, X. H. Li^{63,49}, X. L. Li⁴¹, Xiaoyu Li^{1,54}, Z. Y. Li⁵⁰, H. Liang^{63,49}, H. Liang^{1,54}, H. Liang²⁷, Y. F. Liang⁴⁵, Y. T. Liang²⁵, G. R. Liao¹², L. Z. Liao^{1,54}, J. Libby²¹, C. X. Lin⁵⁰, B. J. Liu¹, C. X. Liu¹, D. Liu^{63,49}, F. H. Liu⁴⁴, Fang Liu¹, Feng Liu⁶, H. B. Liu¹³, H. M. Liu^{1,54}, Huanhuan Liu¹, Huihui Liu¹⁷, J. B. Liu^{63,49}, J. L. Liu⁶⁴, J. Y. Liu^{1,54}, K. Liu¹, K. Y. Liu³³, Ke Liu⁶, L. Liu^{63,49}, M. H. Liu^{9,h}, P. L. Liu¹, Q. Liu⁵⁴, Q. Liu⁶⁸, S. B. Liu^{63,49}, Shuai Liu⁴⁶, T. Liu^{1,54}, W. M. Liu^{63,49}, X. Liu³¹, Y. Liu³¹, Y. B. Liu³⁶, Z. A. Liu^{1,49,54}, Z. Q. Liu⁴¹, X. C. Lou^{1,49,54}, F. X. Lu¹⁶, F. X. Lu⁵⁰, H. J. Lu¹⁸, J. D. Lu^{1,54}, J. G. Lu^{1,49}, X. L. Lu¹, Y. Lu¹, Y. P. Lu^{1,49}, C. L. Luo³⁴, M. X. Luo⁷⁰, P. W. Luo⁵⁰, T. Luo^{9,h}, X. L. Luo^{1,49}, S. Lusso^{66C}, X. R. Lyu⁵⁴, F. C. Ma³³, H. L. Ma¹, L. L. Ma⁴¹, M. M. Ma^{1,54}, Q. M. Ma¹, R. Q. Ma^{1,54}, R. T. Ma⁵⁴, X. X. Ma^{1,54}, X. Y. Ma^{1,49}, F. E. Maas¹⁵, M. Maggiora^{66A,66C}, S. Maldaner⁴, S. Malde⁶¹, Q. A. Malik⁶⁵, A. Mangoni^{23B}, Y. J. Mao^{38,k}, Z. P. Mao¹, S. Marcello^{66A,66C}, Z. X. Meng⁵⁷, J. G. Messchendorp⁵⁵, G. Mezzadri^{24A}, T. J. Min³⁵, R. E. Mitchell²², X. H. Mo^{1,49,54}, Y. J. Mo⁶, N. Yu. Muchnoi^{10,c}, H. Muramatsu⁵⁹, S. Nakhoul^{11,f}, Y. Nefedov²⁹, F. Nerling^{11,f}, I. B. Nikolaev^{10,c}, Z. Ning^{1,49}, S. Nisar^{8,i}, S. L. Olsen⁵⁴, Q. Ouyang^{1,49,54}, S. Pacetti^{23B,23C}, X. Pan^{9,h}, Y. Pan⁵⁸, A. Pathak¹, P. Patteri^{23A}, M. Pelizaeus⁴, H. P. Peng^{63,49}, K. Peters^{11,f}, J. Pettersson⁶⁷, J. L. Ping³⁴, R. G. Ping^{1,54}, R. Poling⁵⁹, V. Prasad^{63,49}, H. Qi^{63,49}, H. R. Qi⁵², K. H. Qi²⁵, M. Qi³⁵, T. Y. Qi⁹, T. Y. Qi², S. Qian^{1,49}, W. B. Qian⁵⁴, Z. Qian⁵⁰, C. F. Qiao⁵⁴, L. Q. Qin¹², X. P. Qin⁹, X. S. Qin⁴¹, Z. H. Qin^{1,49}, J. F. Qiu¹, S. Q. Qu³⁶, K. H. Rashid⁶⁵, K. Ravindran²¹, C. F. Redmer²⁸, A. Rivetti^{66C}, V. Rodin⁵⁵, M. Rolo^{66C}, G. Rong^{1,54}, Ch. Rosner¹⁵, M. Rump⁶⁰, H. S. Sang⁶³, A. Sarantsev^{29,d}, Y. Schelhaas²⁸, C. Schnier⁴, K. Schoenning⁶⁷, M. Scodeggio^{24A,24B}, D. C. Shan⁴⁶, W. Shan¹⁹, X. Y. Shan^{63,49}, J. F. Shangguan⁴⁶, M. Shao^{63,49}, C. P. Shen⁹, P. X. Shen³⁶, X. Y. Shen^{1,54}, H. C. Shi^{63,49}, R. S. Shi^{1,54}, X. Shi^{1,49}, X. D. Shi^{63,49}, J. J. Song⁴¹, W. M. Song^{27,1}, Y. X. Song^{38,k}, S. Sosio^{66A,66C}, S. Spataro^{66A,66C}, K. X. Su⁶⁸, P. P. Su⁴⁶, F. F. Sui⁴¹, G. X. Sun¹, H. K. Sun¹, J. F. Sun¹⁶, L. Sun⁶⁸, S. S. Sun^{1,54}, T. Sun^{1,54}, W. Y. Sun³⁴, W. Y. Sun²⁷, X. Sun^{20,l}, Y. J. Sun^{63,49}, Y. K. Sun^{63,49}, Y. Z. Sun¹, Z. T. Sun¹, Y. H. Tan⁶⁸, Y. X. Tan^{63,49}, C. J. Tang⁴⁵, G. Y. Tang¹, J. Tang⁵⁰, J. X. Teng^{63,49}, V. Thoren⁶⁷, W. H. Tian⁴³, Y. T. Tian²⁵, I. Uman^{53B}, B. Wang¹, C. W. Wang³⁵, D. Y. Wang^{38,k}, H. J. Wang³¹, H. P. Wang^{1,54}, K. Wang^{1,49}, L. L. Wang¹, M. Wang⁴¹, M. Z. Wang^{38,k}, Meng Wang^{1,54}, W. Wang⁵⁰, W. H. Wang⁶⁸, W. P. Wang^{63,49}, X. Wang^{38,k}, X. F. Wang³¹, X. L. Wang^{9,h}, Y. Wang⁵⁰, Y. Wang^{63,49}, Y. D. Wang³⁷, Y. F. Wang^{1,49,54}, Y. Q. Wang¹, Y. Y. Wang³¹, Z. Wang^{1,49}, Z. Y. Wang¹, Ziyi Wang⁵⁴,

Zongyuan Wang^{1,54}, D. H. Wei¹², P. Weidenkaff²⁸, F. Weidner⁶⁰, S. P. Wen¹, D. J. White⁵⁸, U. Wiedner⁴, G. Wilkinson⁶¹, M. Wolke⁶⁷, L. Wollenberg⁴, J. F. Wu^{1,54}, L. H. Wu¹, L. J. Wu^{1,54}, X. Wu^{9,h}, Z. Wu^{1,49}, L. Xia^{63,49}, H. Xiao^{9,h}, S. Y. Xiao¹, Z. J. Xiao³⁴, X. H. Xie^{38,k}, Y. G. Xie^{1,49}, Y. H. Xie⁶, T. Y. Xing^{1,54}, G. F. Xu¹, Q. J. Xu¹⁴, W. Xu^{1,54}, X. P. Xu⁴⁶, Y. C. Xu⁵⁴, F. Yan^{9,h}, L. Yan^{9,h}, W. B. Yan^{63,49}, W. C. Yan⁷¹, Xu Yan⁴⁶, H. J. Yang^{42,g}, H. X. Yang¹, L. Yang⁴³, S. L. Yang⁵⁴, Y. X. Yang¹², Yifan Yang^{1,54}, Zhi Yang²⁵, M. Ye^{1,49}, M. H. Ye⁷, J. H. Yin¹, Z. Y. You⁵⁰, B. X. Yu^{1,49,54}, C. X. Yu³⁶, G. Yu^{1,54}, J. S. Yu^{20,l}, T. Yu⁶⁴, C. Z. Yuan^{1,54}, L. Yuan², X. Q. Yuan^{38,k}, Y. Yuan¹, Z. Y. Yuan⁵⁰, C. X. Yue³², A. Yuncu^{53,A,a}, A. A. Zafar⁶⁵, Y. Zeng^{20,l}, B. X. Zhang¹, Guangyi Zhang¹⁶, H. Zhang⁶³, H. H. Zhang⁵⁰, H. H. Zhang²⁷, H. Y. Zhang^{1,49}, J. J. Zhang⁴³, J. L. Zhang⁶⁹, J. Q. Zhang³⁴, J. W. Zhang^{1,49,54}, J. Y. Zhang¹, J. Z. Zhang^{1,54}, Jianyu Zhang^{1,54}, Jiawei Zhang^{1,54}, L. M. Zhang⁵², L. Q. Zhang⁵⁰, Lei Zhang³⁵, S. Zhang⁵⁰, S. F. Zhang³⁵, Shulei Zhang^{20,l}, X. D. Zhang³⁷, X. Y. Zhang⁴¹, Y. Zhang⁶¹, Y. H. Zhang^{1,49}, Y. T. Zhang^{63,49}, Yan Zhang^{63,49}, Yao Zhang¹, Yi Zhang^{9,h}, Z. H. Zhang⁶, Z. Y. Zhang⁶⁸, G. Zhao¹, J. Zhao³², J. Y. Zhao^{1,54}, J. Z. Zhao^{1,49}, Lei Zhao^{63,49}, Ling Zhao¹, M. G. Zhao³⁶, Q. Zhao¹, S. J. Zhao⁷¹, Y. B. Zhao^{1,49}, Y. X. Zhao²⁵, Z. G. Zhao^{63,49}, A. Zhemchugov^{29,b}, B. Zheng⁶⁴, J. P. Zheng^{1,49}, Y. Zheng^{38,k}, Y. H. Zheng⁵⁴, B. Zhong³⁴, C. Zhong⁶⁴, L. P. Zhou^{1,54}, Q. Zhou^{1,54}, X. Zhou⁶⁸, X. K. Zhou⁵⁴, X. R. Zhou^{63,49}, X. Y. Zhou³², A. N. Zhu^{1,54}, J. Zhu³⁶, K. Zhu¹, K. J. Zhu^{1,49,54}, S. H. Zhu⁶², T. J. Zhu⁶⁹, W. J. Zhu^{9,h}, W. J. Zhu³⁶, Y. C. Zhu^{63,49}, Z. A. Zhu^{1,54}, B. S. Zou¹, J. H. Zou¹

(BESIII Collaboration)

¹ *Institute of High Energy Physics, Beijing 100049, People's Republic of China*

² *Beihang University, Beijing 100191, People's Republic of China*

³ *Beijing Institute of Petrochemical Technology, Beijing 102617, People's Republic of China*

⁴ *Bochum Ruhr-University, D-44780 Bochum, Germany*

⁵ *Carnegie Mellon University, Pittsburgh, Pennsylvania 15213, USA*

⁶ *Central China Normal University, Wuhan 430079, People's Republic of China*

⁷ *China Center of Advanced Science and Technology, Beijing 100190, People's Republic of China*

⁸ *COMSATS University Islamabad, Lahore Campus, Defence Road, Off Raiwind Road, 54000 Lahore, Pakistan*

⁹ *Fudan University, Shanghai 200443, People's Republic of China*

¹⁰ *G.I. Budker Institute of Nuclear Physics SB RAS (BINP), Novosibirsk 630090, Russia*

¹¹ *GSI Helmholtzcentre for Heavy Ion Research GmbH, D-64291 Darmstadt, Germany*

¹² *Guangxi Normal University, Guilin 541004, People's Republic of China*

¹³ *Guangxi University, Nanning 530004, People's Republic of China*

¹⁴ *Hangzhou Normal University, Hangzhou 310036, People's Republic of China*

¹⁵ *Helmholtz Institute Mainz, Johann-Joachim-Becher-Weg 45, D-55099 Mainz, Germany*

¹⁶ *Henan Normal University, Xinxiang 453007, People's Republic of China*

¹⁷ *Henan University of Science and Technology, Luoyang 471003, People's Republic of China*

¹⁸ *Huangshan College, Huangshan 245000, People's Republic of China*

¹⁹ *Hunan Normal University, Changsha 410081, People's Republic of China*

²⁰ *Hunan University, Changsha 410082, People's Republic of China*

²¹ *Indian Institute of Technology Madras, Chennai 600036, India*

²² *Indiana University, Bloomington, Indiana 47405, USA*

²³ *INFN Laboratori Nazionali di Frascati, (A)INFN Laboratori Nazionali di Frascati, I-00044, Frascati, Italy; (B)INFN Sezione di Perugia, I-06100, Perugia, Italy; (C)University of Perugia, I-06100, Perugia, Italy*

²⁴ *INFN Sezione di Ferrara, (A)INFN Sezione di Ferrara, I-44122, Ferrara, Italy; (B)University of Ferrara, I-44122, Ferrara, Italy*

²⁵ *Institute of Modern Physics, Lanzhou 730000, People's Republic of China*

²⁶ *Institute of Physics and Technology, Peace Ave. 54B, Ulaanbaatar 13330, Mongolia*

²⁷ *Jilin University, Changchun 130012, People's Republic of China*

²⁸ *Johannes Gutenberg University of Mainz, Johann-Joachim-Becher-Weg 45, D-55099 Mainz, Germany*

²⁹ *Joint Institute for Nuclear Research, 141980 Dubna, Moscow region, Russia*

³⁰ *Justus-Liebig-Universitaet Giessen, II. Physikalisches Institut, Heinrich-Buff-Ring 16, D-35392 Giessen, Germany*

³¹ *Lanzhou University, Lanzhou 730000, People's Republic of China*

³² *Liaoning Normal University, Dalian 116029, People's Republic of China*

- ³³ Liaoning University, Shenyang 110036, People's Republic of China
- ³⁴ Nanjing Normal University, Nanjing 210023, People's Republic of China
- ³⁵ Nanjing University, Nanjing 210093, People's Republic of China
- ³⁶ Nankai University, Tianjin 300071, People's Republic of China
- ³⁷ North China Electric Power University, Beijing 102206, People's Republic of China
- ³⁸ Peking University, Beijing 100871, People's Republic of China
- ³⁹ Qufu Normal University, Qufu 273165, People's Republic of China
- ⁴⁰ Shandong Normal University, Jinan 250014, People's Republic of China
- ⁴¹ Shandong University, Jinan 250100, People's Republic of China
- ⁴² Shanghai Jiao Tong University, Shanghai 200240, People's Republic of China
- ⁴³ Shanxi Normal University, Linfen 041004, People's Republic of China
- ⁴⁴ Shanxi University, Taiyuan 030006, People's Republic of China
- ⁴⁵ Sichuan University, Chengdu 610064, People's Republic of China
- ⁴⁶ Soochow University, Suzhou 215006, People's Republic of China
- ⁴⁷ South China Normal University, Guangzhou 510006, People's Republic of China
- ⁴⁸ Southeast University, Nanjing 211100, People's Republic of China
- ⁴⁹ State Key Laboratory of Particle Detection and Electronics,
Beijing 100049, Hefei 230026, People's Republic of China
- ⁵⁰ Sun Yat-Sen University, Guangzhou 510275, People's Republic of China
- ⁵¹ Suranaree University of Technology, University Avenue 111, Nakhon Ratchasima 30000, Thailand
- ⁵² Tsinghua University, Beijing 100084, People's Republic of China
- ⁵³ Turkish Accelerator Center Particle Factory Group, (A)Istanbul Bilgi University, 34060 Eyup, Istanbul, Turkey; (B)Near East University, Nicosia, North Cyprus, Mersin 10, Turkey
- ⁵⁴ University of Chinese Academy of Sciences, Beijing 100049, People's Republic of China
- ⁵⁵ University of Groningen, NL-9747 AA Groningen, The Netherlands
- ⁵⁶ University of Hawaii, Honolulu, Hawaii 96822, USA
- ⁵⁷ University of Jinan, Jinan 250022, People's Republic of China
- ⁵⁸ University of Manchester, Oxford Road, Manchester, M13 9PL, United Kingdom
- ⁵⁹ University of Minnesota, Minneapolis, Minnesota 55455, USA
- ⁶⁰ University of Muenster, Wilhelm-Klemm-Str. 9, 48149 Muenster, Germany
- ⁶¹ University of Oxford, Keble Rd, Oxford, UK OX13RH
- ⁶² University of Science and Technology Liaoning, Anshan 114051, People's Republic of China
- ⁶³ University of Science and Technology of China, Hefei 230026, People's Republic of China
- ⁶⁴ University of South China, Hengyang 421001, People's Republic of China
- ⁶⁵ University of the Punjab, Lahore-54590, Pakistan
- ⁶⁶ University of Turin and INFN, (A)University of Turin, I-10125, Turin, Italy; (B)University of Eastern Piedmont, I-15121, Alessandria, Italy; (C)INFN, I-10125, Turin, Italy
- ⁶⁷ Uppsala University, Box 516, SE-75120 Uppsala, Sweden
- ⁶⁸ Wuhan University, Wuhan 430072, People's Republic of China
- ⁶⁹ Xinyang Normal University, Xinyang 464000, People's Republic of China
- ⁷⁰ Zhejiang University, Hangzhou 310027, People's Republic of China
- ⁷¹ Zhengzhou University, Zhengzhou 450001, People's Republic of China
- ^a Also at Bogazici University, 34342 Istanbul, Turkey
- ^b Also at the Moscow Institute of Physics and Technology, Moscow 141700, Russia
- ^c Also at the Novosibirsk State University, Novosibirsk, 630090, Russia
- ^d Also at the NRC "Kurchatov Institute", PNPI, 188300, Gatchina, Russia
- ^e Also at Istanbul Arel University, 34295 Istanbul, Turkey
- ^f Also at Goethe University Frankfurt, 60323 Frankfurt am Main, Germany
- ^g Also at Key Laboratory for Particle Physics, Astrophysics and Cosmology, Ministry of Education; Shanghai Key Laboratory for Particle Physics and Cosmology; Institute of Nuclear and Particle Physics, Shanghai 200240, People's Republic of China

^h Also at Key Laboratory of Nuclear Physics and Ion-beam Application (MOE) and Institute of Modern Physics, Fudan University, Shanghai 200443, People's Republic of China

ⁱ Also at Harvard University, Department of Physics, Cambridge, MA, 02138, USA

^j Currently at: Institute of Physics and Technology, Peace Ave.54B, Ulaanbaatar 13330, Mongolia

^k Also at State Key Laboratory of Nuclear Physics and Technology,

Peking University, Beijing 100871, People's Republic of China

^l School of Physics and Electronics, Hunan University, Changsha 410082, China

^m Also at Guangdong Provincial Key Laboratory of Nuclear Science, Institute of Quantum Matter, South China Normal University, Guangzhou 510006, China

Using 2.93 fb^{-1} of e^+e^- collision data taken with the BESIII detector at a center-of-mass energy of 3.773 GeV, the observation of the $D^0 \rightarrow K_1(1270)^- e^+ \nu_e$ semileptonic decay is presented. The statistical significance of the decay $D^0 \rightarrow K_1(1270)^- e^+ \nu_e$ is greater than 10σ . The branching fraction of $D^0 \rightarrow K_1(1270)^- e^+ \nu_e$ is measured to be $(1.09 \pm 0.13_{-0.13}^{+0.09} \pm 0.12) \times 10^{-3}$. Here, the first uncertainty is statistical, the second is systematic, and the third originates from the assumed branching fraction of $K_1(1270)^- \rightarrow K^- \pi^+ \pi^-$.

PACS numbers: 13.20.Fc, 12.15.Hh

Semileptonic (SL) D decays offer a good testbed to understand nonperturbative strong-interaction dynamics in weak decays [1, 2]. Studies of the SL $D^{0(+)}$ decays into the strange axial-vector mesons $K_1(1270)$ or $K_1(1400)$ are especially appealing. Reference [3] points out that the combined measurements of $D^{0(+)} \rightarrow \bar{K}_1(1270)\ell^+\nu_\ell$ and $B \rightarrow K_1(1270)\gamma$ provide a possible way to determine the photon polarization in $b \rightarrow s\gamma$ transitions without considerable theoretical ambiguity. Knowledge of the $b \rightarrow s\gamma$ photon polarization plays a unique role in probing right-handed couplings in new physics [3–5]. Throughout this Letter, charged conjugated modes are always implied.

To date, the $K_1(1270)$ and $K_1(1400)$ mesons have been extensively investigated in τ , D , B , and charmonium decays [6–15]. In theory, the physical mass eigenstates of $K_1(1270)$ and $K_1(1400)$ mesons are decomposed as mixtures of the 1P_1 and 3P_1 states with a mixing angle θ_{K_1} . Various approaches were proposed to extract θ_{K_1} , but with very different results [16–23]. Experimental measurements of $D^{0(+)} \rightarrow \bar{K}_1(1270)e^+\nu_e$ offer deeper insight into the mixing angle θ_{K_1} , which is essential for reliable calculations describing the τ [16], B [18, 24], and D [25, 26] decays involving K_1 , and for investigations in the field of hadron spectroscopy [27].

The branching fractions (BFs) of $D^{0(+)} \rightarrow \bar{K}_1(1270)e^+\nu_e$ have been computed with different models: the Isgur-Scora-Grinstein-Wise (ISGW) quark model [1] and its update, ISGW2 [2], three-point QCD sum rules (3PSR) [28], covariant light-front quark model (CLFQM) [29], and the light-cone QCD sum rules (LCSR) [30, 31]. The predicted BFs, which are sensitive to θ_{K_1} and its sign, vary from 10^{-3} to 10^{-2} [28, 29, 31]. Measurements of these decay BFs are the key to testing different theoretical calculations and understanding the weak-decay mechanisms of D mesons. For example, assuming isospin symmetry, the ratio of

the partial decay widths for the SL $D^{0(+)}$ decays, which are both mediated via $c \rightarrow se^+\nu_e$, is expected to be unity [32]. Measuring the BFs thus allows a test of isospin invariance in $D^{0(+)} \rightarrow \bar{K}_1(1270)e^+\nu_e$. Large $D^{0(+)} \rightarrow \bar{K}_1(1270)\ell^+\nu_\ell$ samples also supply a clean environment, with no additional hadrons in the final state, to accurately determine the mass and width of $K_1(1270)$ meson, and to explore the relative strengths and phases of $K_1(1270)$ decays into various final states, which currently all suffer large uncertainties.

An observation of $D^+ \rightarrow \bar{K}_1(1270)^0 e^+ \nu_e$ was previously reported by BESIII [33]. However, the only evidence for $D^0 \rightarrow K_1(1270)^- e^+ \nu_e$ was reported by CLEO [34]. This Letter presents an observation of $D^0 \rightarrow K_1(1270)^- e^+ \nu_e$ by using an e^+e^- data sample corresponding to an integrated luminosity of 2.93 fb^{-1} [35] recorded at a center-of-mass energy of 3.773 GeV with the BESIII detector [36].

Details about the design and performance of the BESIII detector are given in Ref. [36]. Simulated samples produced with a GEANT4-based [37] Monte Carlo (MC) package, which includes the geometric description of the BESIII detector and the detector response, are used to determine the detection efficiency and to estimate the backgrounds. The simulation includes the beam-energy spread and initial-state radiation (ISR) in the e^+e^- annihilations modeled with the generator KKMC [38]. The inclusive MC samples consist of the production of the $D\bar{D}$ pairs, the non- $D\bar{D}$ decays of the $\psi(3770)$, the ISR production of the J/ψ and $\psi(3686)$ states, and the continuum processes incorporated in KKMC [38]. The known decay modes are modeled with EVTGEN [39] using BFs taken from the Particle Data Group [40], and the remaining unknown decays from the charmonium states with LUNDCHARM [41]. Final-state radiation (FSR) from charged final-state particles is incorporated with the PHOTOS package [42]. The $D^0 \rightarrow K_1(1270)^- e^+ \nu_e$

decay is simulated with the ISGW2 model [43] and the $K_1(1270)^-$ meson is allowed to decay into all intermediate processes that result in a $K^-\pi^+\pi^-$ final state. The resonance shape of the $K_1(1270)^-$ meson is parameterized by a relativistic Breit-Wigner function, and the mass and width of $K_1(1270)^-$ meson are fixed at the world-average values (1.253 ± 0.007) GeV/ c^2 and (90 ± 20) MeV, respectively [40]. The BF's of $K_1(1270)^-$ meson subdecays measured by Belle [44] are input to generate the signal MC events, since they give better consistency between data and MC simulation than those reported in Ref. [40].

The measurement employs the $e^+e^- \rightarrow \psi(3770) \rightarrow D^0\bar{D}^0$ decay chain. The \bar{D}^0 mesons are reconstructed by their hadronic decays to $\bar{D}^0 \rightarrow K^+\pi^-$, $K^+\pi^-\pi^0$, and $K^+\pi^-\pi^-\pi^+$. These inclusively selected events are referred to as single-tag (ST) \bar{D}^0 mesons. In the presence of the ST \bar{D}^0 mesons, candidates for $D^0 \rightarrow K_1(1270)^-e^+\nu_e$ are selected to form double-tag (DT) events. For a given tag mode, the BF of $D^0 \rightarrow K_1(1270)^-e^+\nu_e$, \mathcal{B}_{SL} , is obtained by

$$\mathcal{B}_{\text{SL}} = N_{\text{DT}} / (N_{\text{ST}} \cdot \varepsilon_{\text{SL}} \cdot \mathcal{B}_{\text{sub}}), \quad (1)$$

where N_{ST} and N_{DT} are the ST and DT yields in the data sample, $\varepsilon_{\text{SL}} = \varepsilon_{\text{DT}}/\varepsilon_{\text{ST}}$ is the efficiency of detecting the SL decay in the presence of the ST \bar{D}^0 meson, and \mathcal{B}_{sub} is the BF of $K_1(1270)^- \rightarrow K^-\pi^+\pi^-$. ε_{ST} and ε_{DT} are the ST and DT efficiencies of selecting the ST and DT candidates, respectively.

All charged tracks must originate from the interaction point with a distance of closest approach less than 1 cm in the transverse plane and less than 10 cm along the axis of the multilayer drift chamber (MDC). Their polar angles (θ) are required to satisfy $|\cos\theta| < 0.93$. Charged particle identification (PID) of charged kaons and pions is performed by combining the time-of-flight (TOF) information and the specific ionization energy loss (dE/dx) measured in the MDC. Positron PID uses the combined information from the dE/dx , TOF, and electromagnetic calorimeter (EMC). The combined confidence levels under the positron, pion, and kaon hypotheses (CL_e , CL_π and CL_K , respectively) are calculated. Kaon (pion) candidates are required to satisfy $CL_K > CL_\pi$ ($CL_\pi > CL_K$). Positron candidates are required to satisfy $CL_e / (CL_e + CL_\pi + CL_K) > 0.8$. To reduce the background from hadrons and muons, the positron candidate is further required to have a deposited energy in the EMC greater than 0.8 times its momentum in the MDC. The π^0 meson is reconstructed via $\pi^0 \rightarrow \gamma\gamma$ decay. The energy deposited in the EMC of each photon is required to be greater than 25 MeV in the barrel ($|\cos\theta| < 0.80$) region or 50 MeV in the end caps ($0.86 < |\cos\theta| < 0.92$) region, and the shower time has to be within 700 ns of the event start time. Pairings with both photons from the end caps are rejected because of

poor resolution. The $\gamma\gamma$ combination with an invariant mass in the range $(0.115, 0.150)$ GeV/ c^2 are regarded as π^0 candidates, and a kinematic fit by constraining the $\gamma\gamma$ invariant mass to the π^0 nominal mass [40] is performed to improve the mass resolution. For $\bar{D}^0 \rightarrow K^+\pi^-$, the backgrounds from cosmic ray events, radiative Bhabha scattering, and dimuon events are suppressed with the same requirements as used in Ref. [45].

The ST \bar{D}^0 mesons are identified by the energy difference $\Delta E \equiv E_{\bar{D}^0} - E_{\text{beam}}$ and the beam-constrained mass $M_{\text{BC}} \equiv \sqrt{E_{\text{beam}}^2 - |\vec{p}_{\bar{D}^0}|^2}$, where E_{beam} is the beam energy, and $E_{\bar{D}^0}$ and $\vec{p}_{\bar{D}^0}$ are the total energy and momentum of the ST \bar{D}^0 in the e^+e^- rest frame. If there are multiple combinations in an event, the combination with the smallest $|\Delta E|$ is chosen for each tag mode. The combinatorial backgrounds in the M_{BC} distributions are suppressed by requiring ΔE within $(-29, 27)$, $(-69, 38)$, and $(-31, 28)$ MeV for $\bar{D}^0 \rightarrow K^+\pi^-$, $K^+\pi^-\pi^0$, and $K^+\pi^-\pi^-\pi^+$, respectively, which correspond to about 3.5σ away from the fitted peak.

The M_{BC} distributions of the accepted ST candidates in the data sample for the three tag modes are shown in Fig. 1. To extract the ST yield for each tag mode, an unbinned maximum-likelihood fit is performed to the corresponding M_{BC} distribution. The signal is described by the MC-simulated shape convolved with a double-Gaussian function accounting for the resolution difference between data and MC simulation, and the background is modeled by an ARGUS function [46]. Fit results are shown in Fig. 1. Events within $M_{\text{BC}} \in (1.858, 1.874)$ GeV/ c^2 are kept for further analysis. The ST yields for the $\bar{D}^0 \rightarrow K^+\pi^-$, $K^+\pi^-\pi^0$, and $K^+\pi^-\pi^-\pi^+$ tag modes are $542153 \pm 774_{\text{stat}}$, $1080690 \pm 1727_{\text{stat}}$, and $737036 \pm 1712_{\text{stat}}$, respectively.

Particles recoiling against the ST \bar{D}^0 meson candidates are used to reconstruct candidates for $D^0 \rightarrow K_1(1270)^-e^+\nu_e$ decay. It is required that there are only four good unused charged tracks available for this selection. The $K_1(1270)^-$ meson is reconstructed using its dominant decay $K_1(1270)^- \rightarrow K^-\pi^+\pi^-$. The charge of the lepton candidate is required to be the same as that of the charged kaon of tag side. The other three charged tracks are identified as a kaon and two pions, based on the same PID criteria used for the ST. The kaon candidate must have charge opposite to that of the positron.

Additional criteria that have been optimized by analyzing the inclusive MC sample are further introduced to suppress backgrounds. To distinguish positrons from backgrounds related to hadrons, the positron candidates are required to satisfy the requirement of $E/p - 0.38 > 0.14 \times \chi_{dE/dx}^e$, where E , p , and $\chi_{dE/dx}^e$ are the energy deposited in the EMC, the momentum measured by the MDC, and the standard deviation between the measured and expected dE/dx with the positron hypothesis, respectively. To suppress the background from $D^0 \rightarrow K^-\pi^+\pi^-\pi^+$, we require $M_{K^-\pi^+\pi^-\pi^+} < 1.8$ GeV/ c^2 ,

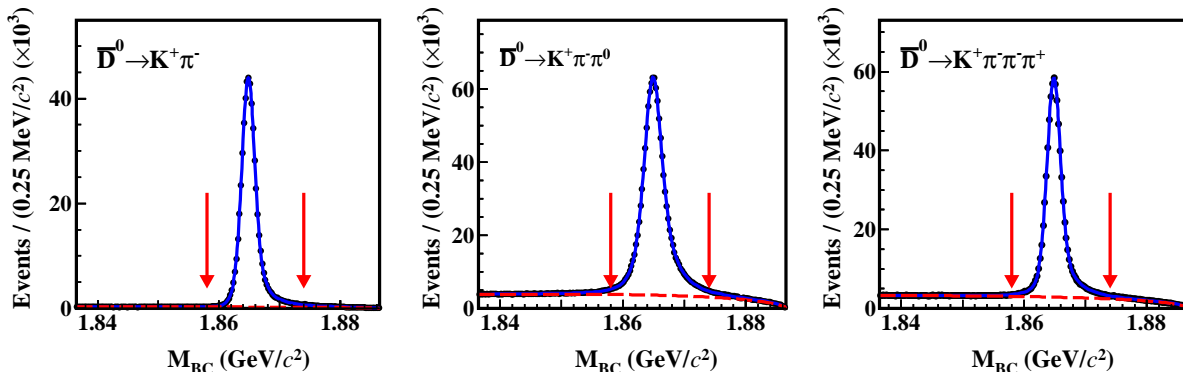


Fig. 1. Fits to the M_{BC} distributions of the ST candidates in data. Points with error bars are data. Blue solid curves are the fit results and red dashed curves represent the background contributions of the fit. The pair of red arrows in each subfigure indicate the M_{BC} window.

where $\pi_{e \rightarrow \pi}^+$ is the positron candidate reconstructed with the pion mass hypothesis. To suppress the background from $D^0 \rightarrow K^- \pi^+ \pi^0$ ($\pi^0 \rightarrow e^+ e^- \gamma$ and missing another π^0), the opening angle between e^+ and π^- (θ_a) is required to satisfy $\cos \theta_a < 0.94$. To suppress the background from $D^0 \rightarrow K^- \pi^+ \pi^- \pi^+ \pi^0$, we require $M_{K^- \pi^+ \pi^- \pi^+ \pi^0} < 1.4 \text{ GeV}/c^2$ when there is at least one reconstructed π^0 among the photons recoiling against the ST \bar{D}^0 meson in an event. Furthermore, the opening angle between the missing momentum (defined below) and the most energetic unused shower (θ_b) is required to satisfy $\cos \theta_b < 0.81$. To suppress the background from $D^0 \rightarrow K^- \pi^0 e^+ \nu_e$ with $\pi^0 \rightarrow e^+ e^- \gamma$, we require $M_{\pi^+ \pi^-} > 0.31 \text{ GeV}/c^2$. Background involving K_S^0 decay is suppressed by requiring $M_{\pi^+ \pi^-}$ outside the interval (0.488, 0.508) GeV/c^2 . For the $\bar{D}^0 \rightarrow K^+ \pi^- \pi^0$ tag mode, combinatorial background from $D^- \rightarrow K^+ \pi^- \pi^-$ vs. $D^+ \rightarrow K^- \pi^+ X$ is suppressed by requiring the difference between the beam-energy and the energy of the $(K^+ \pi^-)_{\text{tag}} \pi_{\text{sig}}^-$ combination to be greater than 8 MeV.

Information concerning the undetectable neutrino is inferred by the kinematic quantity $M_{\text{miss}}^2 \equiv E_{\text{miss}}^2 - |\vec{p}_{\text{miss}}|^2$, where E_{miss} and \vec{p}_{miss} are the missing energy and momentum of the SL candidate, respectively, calculated by $E_{\text{miss}} \equiv E_{\text{beam}} - \sum_j E_j$ and $\vec{p}_{\text{miss}} \equiv -\vec{p}_{\bar{D}^0} - \sum_j \vec{p}_j$ in the $e^+ e^-$ center-of-mass frame. The index j sums over the K^- , π^+ , π^- and e^+ of the signal candidate, and E_j and \vec{p}_j are the energy and momentum of the j -th particle, respectively. To partially recover the energy lost to FSR and bremsstrahlung, the four-momenta of photon(s) within 5° of the initial positron direction are added to the positron four-momentum measured by the MDC. To improve the M_{miss}^2 resolution, all the candidate tracks plus the missing neutrino are subjected to a 4-constraint kinematic fit requiring energy and momentum conservation, as well as the invariant masses of the \bar{D}^0 and D^0 candidate particles being constrained to the nominal D^0 mass. The momenta from the kinematic fit

are used to calculate M_{miss}^2 .

Figure 2(a) shows the distribution of $M_{K^- \pi^+ \pi^-}$ vs. M_{miss}^2 of the accepted $D^0 \rightarrow K^- \pi^+ \pi^- e^+ \nu_e$ candidate events in the data sample after combining all tag modes. A clear signal, which concentrates around the $K_1(1270)^-$ nominal mass in the $M_{K^- \pi^+ \pi^-}$ distribution and around zero in the M_{miss}^2 distribution, can be seen. The DT yield is obtained from a two-dimensional (2D) unbinned extended maximum-likelihood simultaneous fit to the data for the three tags. Due to the limited data set, the components of $D^0 \rightarrow K_1(1400)^- e^+ \nu_e$, $D^0 \rightarrow K^*(1410)^- e^+ \nu_e$, $D^0 \rightarrow K_2^*(1430)^- e^+ \nu_e$, and $D^0 \rightarrow (K^- \pi^+ \pi^-)_{\text{non-resonance}} e^+ \nu_e$ are all ignored in this analysis. In the fit, the 2D signal shape is described by the MC-simulated shape extracted from the signal MC events of $D^0 \rightarrow K_1(1270)^- e^+ \nu_e$. The 2D shapes of the peaking background of $D^0 \rightarrow K^- \pi^+ \pi^+ \pi^-$ and the other backgrounds are modeled by those derived from the inclusive MC sample. The number of peaking background events from $D^0 \rightarrow K^- \pi^+ \pi^+ \pi^-$ is fixed at the simulated value, and the number of the other backgrounds is a free parameter. The smooth 2D probability density functions of signal and background are modeled by using RooNDKeysPdf [47, 48]. The signal efficiencies with the ST modes $\bar{D}^0 \rightarrow K^+ \pi^-$, $K^+ \pi^- \pi^0$, and $K^+ \pi^- \pi^- \pi^+$ are $(14.08 \pm 0.14_{\text{stat}})\%$, $(13.38 \pm 0.10_{\text{stat}})\%$, and $(11.22 \pm 0.10_{\text{stat}})\%$, respectively. The BFs given by the three tags are constrained to have the same value in the fit. The 2D fit projections to the M_{miss}^2 and $M_{K^- \pi^+ \pi^-}$ distributions are shown in Figs. 2(b) and 2(c), respectively. From the fit, we obtain the DT yield of $N_{\text{DT}} = 109.0 \pm 12.5_{\text{stat}}$. The statistical significance of the signal is estimated to be greater than 10σ , by comparing the likelihoods with and without the signal component, and taking the change in the number of degrees of freedom into account. The fitted product of the BFs for $D^0 \rightarrow K_1(1270)^- e^+ \nu_e$ and

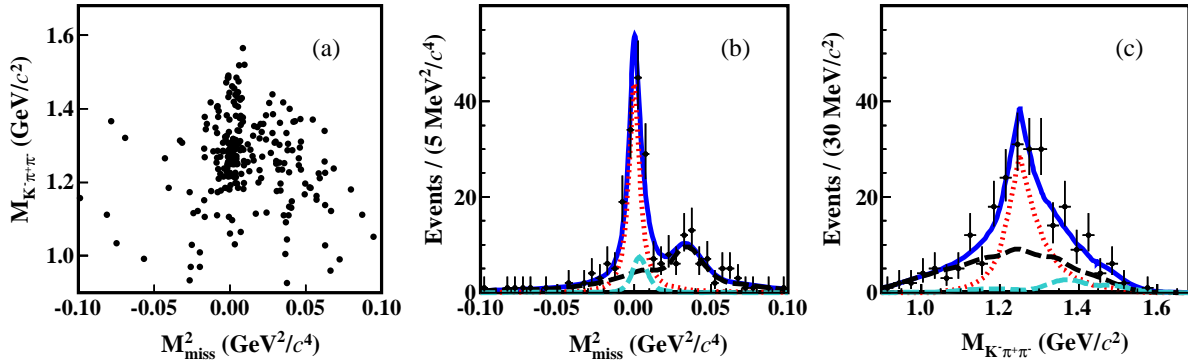


Fig. 2. (a) Distribution of $M_{K^-\pi^+\pi^-}$ vs. M_{miss}^2 of the DT candidate events. Projections of the 2D fit to (b) M_{miss}^2 and (c) $M_{K^-\pi^+\pi^-}$. The distributions are summed over all three tags. In (b) and (c), points with error bars are data; blue solid, red dotted, green dashed, and black dashed curves are total fit, signal, peaking background of $D^0 \rightarrow K^-\pi^+\pi^+\pi^-\pi^0$, and other background, respectively. In (b), the peaking background concentrating around $0.033 \text{ GeV}^2/c^4$ is from $D^0 \rightarrow K^-\pi^+\pi^+\pi^-\pi^0$.

$K_1(1270)^- \rightarrow K^-\pi^+\pi^-$ is

$$\mathcal{B}_{\text{SL}} \cdot \mathcal{B}_{\text{sub}} = (3.59 \pm 0.41_{-0.44}^{+0.31}) \times 10^{-4},$$

where the first and second uncertainties are statistical and systematic, respectively. The reliability of the MC simulation is verified since the data distributions of momenta and $\cos\theta$ of K^- , π^+ , π^- and e^+ as well as invariant masses of $K^-\pi^+$ and $\pi^+\pi^-$ are consistent with those of MC simulations.

The systematic uncertainties relative to the measured BF are discussed below. The DT method ensures that most uncertainties arising from the ST selection cancel. The uncertainty from the ST yield is assigned to be 0.5%, by examining the relative change in the yield between data and MC simulation after varying the signal shape and the endpoint of the ARGUS function in the yield fits.

The systematic uncertainties originating from e^+ tracking and PID efficiencies are studied by using the control samples of $e^+e^- \rightarrow \gamma e^+e^-$ events and those for K^- and π^\pm are investigated with the DT $D\bar{D}$ hadronic events. The e^+ efficiencies for tracking and PID are also re-weighted in 2D (momentum and $\cos\theta$) to match those of the $D^0 \rightarrow K_1(1270)^-e^+\nu_e$ data. For K^- and π^+ , similar weighting is performed on momentum only since the data and MC angular distributions already agree well. Small differences between the data and MC efficiencies for K^- tracking, e^+ tracking, and e^+ PID are found, which are $+(2.6 \pm 0.4)\%$, $+(1.0 \pm 0.2)\%$, and $-(1.4 \pm 0.2)\%$, respectively. The MC efficiencies, corrected by the aforementioned differences, are used for the BF determination. After corrections, the residual uncertainties related to the tracking (PID) efficiencies of e^+ , K^- , π^+ , and π^- are assigned as 0.2% (0.2%), 0.4% (0.3%), 0.2% (0.2%), and 0.2% (0.2%), respectively.

Any systematic effects related to the requirements on $M_{K^-\pi^+\pi^-\pi^+\pi^0}$, $M_{K^-\pi^+\pi^-\pi^+\pi^0}$, $M_{\pi^+\pi^-}$, $\Delta E[(K^-\pi^+)_{\text{tag}}\pi_{\text{sig}}^+]$, $\cos\theta_a$, $\cos\theta_b$, are examined by

varying individual requirements by $\pm 0.05 \text{ GeV}/c^2$, $\pm 0.05 \text{ GeV}/c^2$, $\pm 0.01 \text{ GeV}/c^2$, $\pm 0.004 \text{ GeV}$, ± 0.02 , and ± 0.02 , respectively. Accounting for correlations in the samples, the changes in the BFs are smaller than the statistical uncertainty on the difference, so neither a systematic correction nor uncertainty is applied from this source according to Ref. [49]. The effect of the input BFs from $K_1(1270)^-$ meson subdecays on the signal efficiencies is estimated by varying each of the subdecay BFs of Belle [44] by $\pm 1\sigma$ and by comparing our nominal signal efficiency to the one based on the world average BFs of $K_1(1270)^-$ meson decays. The quadratic sum of the two variations in the detection efficiency, 3.0%, is assigned as the related systematic uncertainty.

The systematic uncertainty of the 2D fit is estimated to be $^{+6.9\%}_{-11.1\%}$ by examining the BF changes with alternative signal and background shapes. The uncertainty from the signal shape is mainly caused by varying the $K_1(1270)$ width by $\pm 1\sigma$. The uncertainty of background shape is mainly due to non- $K_1(1270)^-$ sources of $K^-\pi^+\pi^-$. It is assigned to be the change of the fitted DT yield after fixing a non-resonant component by referring to the non-resonant fraction in $B \rightarrow J/\psi \bar{K} \pi \pi$ [44]. The uncertainty due to the MC samples' limited size, 1.0%, is considered as a source of systematic uncertainty.

The uncertainty from FSR recovery is assigned to be 0.3% based on studies of a large sample of $D^0 \rightarrow K^-e^+\nu_e$ [50]. The uncertainty due to the kinematic fit is ignored since it is only used to improve the M_{miss}^2 resolution. The total systematic uncertainty is estimated to be $^{+8.7\%}_{-12.3\%}$ by adding all the individual contributions in quadrature.

Using the world average of $\mathcal{B}_{\text{sub}} = (32.9 \pm 3.6)\%$ [40, 51], we obtain

$$\mathcal{B}_{\text{SL}} = \mathcal{B}_{D^0 \rightarrow K_1(1270)^-e^+\nu_e} = (1.09 \pm 0.13_{-0.13}^{+0.09} \pm 0.12) \times 10^{-3},$$

where the third uncertainty is from the external

uncertainty of the assumed BF \mathcal{B}_{sub} .

In summary, using an e^+e^- collision data sample of 2.93 fb^{-1} taken at a center-of-mass energy of 3.773 GeV , we report the first observation of $D^0 \rightarrow K_1(1270)^- e^+ \nu_e$. The obtained product of the BFs for $D^0 \rightarrow K_1(1270)^- e^+ \nu_e$ and $K_1(1270)^- \rightarrow K^- \pi^+ \pi^-$ is consistent with the CLEO's result but with precision improved by about threefold [34]. Our BF of $D^0 \rightarrow K_1(1270)^- e^+ \nu_e$ contributes $(1.68 \pm 0.35)\%$ of the total SL decay width of D^0 [40], which lies between the ISGW prediction (1%) and the ISGW2 prediction (2%), consistent with the BESIII results for the D^+ counterpart [33]. Our BF of $D^0 \rightarrow K_1(1270)^- e^+ \nu_e$ agrees with the CLFQM and LCSR predictions when $\theta_{K_1} \approx 33^\circ$ or 57° [29, 30] and clearly disfavors the prediction reported in Ref. [31]. Using the BF of $D^+ \rightarrow \bar{K}_1(1270)^0 e^+ \nu_e$ measured by BESIII [33] and the world-average lifetimes of D^0 and D^+ [40], we determine the ratio of the partial decay widths of the two decays to be $\Gamma_{D^0 \rightarrow K_1(1270)^- e^+ \nu_e} / \Gamma_{D^+ \rightarrow \bar{K}_1(1270)^0 e^+ \nu_e} = 1.20 \pm 0.20 \pm 0.14 \pm 0.04$, where the systematic uncertainties from the background shape, the tracking and PID efficiencies of K^- , π^+ , and e^+ as well as FSR recovery are canceled, the uncertainties of the lifetimes of D^0 and D^+ are included; the uncertainties of the quoted BFs for $K_1(1270)$ meson decays are largely canceled. This result agrees with unity as predicted by isospin symmetry.

Observation of $\bar{K}_1(1270)$ mesons in the clean environment of SL $D^{0(+)}$ decays opens up the opportunity to further determine the nature of these axial-vector mesons. Studies of the $K\pi\pi$ hadronic system with larger $D^{0(+)} \rightarrow \bar{K}_1(1270) e^+ \nu_e$ samples anticipated at BESIII [52] in the near future will allow for deeper explorations of the production, mass, width, and mixing angle of the $\bar{K}_1(1270)$ meson, as well as provide access to hadronic-transition form factors. Moreover, joint analyses with high statistics samples of $D^{0(+)} \rightarrow \bar{K}_1(1270) \ell^+ \nu_\ell$ at the future super τ -charm factories [53, 54] and $B \rightarrow K_1(1270) \gamma$ samples at Belle II [55] and LHCb [56] will be able to determine the photon polarization in $b \rightarrow s \gamma$ transitions with high accuracy, and thereby over-constrain the right-handed couplings in new physics models.

The BESIII collaboration thanks the staff of BEPCII and the IHEP computing center for their strong support. This work is supported in part by National Key Research and Development Program of China under Contracts Nos. 2020YFA0406300, 2020YFA0406400; National Natural Science Foundation of China (NSFC) under Contracts Nos. 11775230, 11605124, 11625523, 11635010, 11735014, 11822506, 11835012, 11935015, 11935016, 11935018, 11961141012; the Chinese Academy of Sciences (CAS) Large-Scale Scientific Facility Program; Joint Large-Scale Scientific Facility Funds of the NSFC and CAS under Contracts Nos. U1732263, U1832207, U1932108; CAS Key Research Program of

Frontier Sciences under Contracts Nos. QYZDJ-SSW-SLH003, QYZDJ-SSW-SLH040; 100 Talents Program of CAS; INPAC and Shanghai Key Laboratory for Particle Physics and Cosmology; ERC under Contract No. 758462; European Union Horizon 2020 research and innovation programme under Contract No. Marie Skłodowska-Curie grant agreement No 894790; German Research Foundation DFG under Contracts Nos. 443159800, Collaborative Research Center CRC 1044, FOR 2359, GRK 214; Istituto Nazionale di Fisica Nucleare, Italy; Ministry of Development of Turkey under Contract No. DPT2006K-120470; National Science and Technology fund; Olle Engkvist Foundation under Contract No. 200-0605; STFC (United Kingdom); The Knut and Alice Wallenberg Foundation (Sweden) under Contract No. 2016.0157; The Royal Society, UK under Contracts Nos. DH140054, DH160214; The Swedish Research Council; U. S. Department of Energy under Contracts Nos. DE-FG02-05ER41374, DE-SC-0012069.

-
- [1] N. Isgur, D. Scora, B. Grinstein, and M. B. Wise, *Phys. Rev. D* **39**, 799 (1989).
 - [2] D. Scora and N. Isgur, *Phys. Rev. D* **52**, 2783 (1995).
 - [3] W. Wang, F. S. Yu, and Z. X. Zhao, *Phys. Rev. Lett.* **125**, 051802 (2020).
 - [4] D. Atwood, M. Gronau, and A. Soni, *Phys. Rev. Lett.* **79**, 185 (1997).
 - [5] D. Becirevic, E. Kou, A. Le Yaouanc, and A. Tayduganov, *J. High Energy Phys.* **08** (2012) 090.
 - [6] R. Barate *et al.* (ALEPH Collaboration), *Eur. Phys. J. C* **11**, 599 (1999).
 - [7] G. Abbiendi *et al.* (OPAL Collaboration), *Eur. Phys. J. C* **13**, 197 (2000).
 - [8] D. M. Asner *et al.* (CLEO Collaboration), *Phys. Rev. D* **62**, 072006 (2000).
 - [9] K. Abe *et al.* (Belle Collaboration), *Phys. Rev. Lett.* **87**, 161601 (2001).
 - [10] H. Yang *et al.* (Belle Collaboration), *Phys. Rev. Lett.* **94**, 111802 (2005).
 - [11] J. M. Link *et al.* (FOCUS Collaboration), *Phys. Lett. B* **610**, 225 (2005).
 - [12] J. Z. Bai *et al.* (BES Collaboration), *Phys. Rev. Lett.* **83**, 1918 (1999).
 - [13] M. Ablikim *et al.* (BES Collaboration), *Phys. Rev. D* **72**, 092002 (2005).
 - [14] C. Daum *et al.* (ACCMOR Collaboration), *Nucl. Phys. B* **187**, 1 (1981).
 - [15] D. Aston *et al.*, *Nucl. Phys. B* **292**, 693 (1987).
 - [16] M. Suzuki, *Phys. Rev. D* **47**, 1252 (1993).
 - [17] F. Divotgey, L. Olbrich and F. Giacosa, *Eur. Phys. J. A* **49**, 135 (2013).
 - [18] H. Hatanaka and K. C. Yang, *Phys. Rev. D* **77**, 094023 (2008); **77**, 094023(E) (2008).
 - [19] H. Y. Cheng, *Phys. Lett. B* **707**, 116 (2012).
 - [20] H. G. Blundell, S. Godfrey and B. Phelps, *Phys. Rev. D* **53**, 3712 (1996).
 - [21] A. Tayduganov, E. Kou and A. Le Yaouanc, *Phys. Rev.*

- D **55**, 074011 (2012).
- [22] H. J. Lipkin, *Phys. Lett. B* **72**, 249 (1977).
- [23] L. Burakovsky and T. Goldman, *Phys. Rev. D* **56**, 1368 (1997).
- [24] H. Y. Cheng and C. K. Chua, *Phys. Rev. D* **69**, 094007 (2004). **81**, 059901(E) (2010).
- [25] H. Y. Cheng and C. W. Chiang, *Phys. Rev. D* **81**, 074031 (2010).
- [26] H. Y. Cheng, *Phys. Rev. D* **67**, 094007 (2004).
- [27] L. Burakovsky and T. Goldman, *Phys. Rev. D* **57**, 2879 (1998).
- [28] R. Khosravi, K. Azizi, and N. Ghahramany, *Phys. Rev. D* **79**, 036004 (2008).
- [29] H. Y. Cheng and X. W. Kang, *Eur. Phys. J. C* **77**, 587 (2017); **77**, 863(E) (2017), and private communication.
- [30] S. Momeni, *Eur. Phys. J. C* **80**, 553 (2020).
- [31] S. Momeni and R. Khosravi, *J. Phys. G* **46**, 105006 (2019).
- [32] M. A. Ivanov, J. G. Körner, J. N. Pandya, P. Santorelli, N. R. Soni, and C. T. Tran, *Front. Phys. (Beijing)* **14**, 64401 (2019).
- [33] M. Ablikim *et al.* (BESIII Collaboration), *Phys. Rev. Lett.* **123**, 231801 (2020).
- [34] M. Artuso *et al.* (CLEO Collaboration), *Phys. Rev. Lett.* **99**, 191801 (2007).
- [35] M. Ablikim *et al.* (BESIII Collaboration), *Chin. Phys. C* **37**, 123001 (2013); *Phys. Lett. B* **753**, 629 (2016).
- [36] M. Ablikim *et al.* (BESIII Collaboration), *Nucl. Instrum. Meth. A* **614**, 345 (2010).
- [37] S. Agostinelli *et al.* (GEANT4 Collaboration), *Nucl. Instrum. Meth. A* **506**, 250 (2003).
- [38] S. Jadach, B. F. L. Ward, and Z. Was, *Comp. Phys. Comm.* **130**, 260 (2000); *Phys. Rev. D* **63**, 113009 (2001).
- [39] D. J. Lange, *Nucl. Instrum. Meth. A* **462**, 152 (2001); R. G. Ping, *Chin. Phys. C* **32**, 599 (2008).
- [40] P. A. Zyla *et al.* (Particle Data Group), *Prog. Theor. Exp. Phys.* **2020**, 083C01 (2020).
- [41] J. C. Chen, G. S. Huang, X. R. Qi, D. H. Zhang, and Y. S. Zhu, *Phys. Rev. D* **62**, 034003 (2000).
- [42] E. Richter-Was, *Phys. Lett. B* **303**, 163 (1993).
- [43] D. Becirevic and A. B. Kaidalov, *Phys. Lett. B* **478**, 417 (2000).
- [44] H. Guler *et al.* (Belle Collaboration), *Phys. Rev. D* **83**, 032005 (2011).
- [45] M. Ablikim *et al.* (BESIII Collaboration), *Phys. Lett. B* **734**, 227 (2014).
- [46] H. Albrecht *et al.* (ARGUS Collaboration), *Phys. Lett. B* **241**, 278 (1990).
- [47] W. Verkerke and D. Kirkby, *eConf* No. C0303241, MOLT007 (2003), [arXiv:physics/0306116].
- [48] <https://root.cern.ch/doc/master/classRooNDKeysPdf.html>.
- [49] R. Barlow *et al.*, arXiv:0207026[hep-ex].
- [50] M. Ablikim *et al.* (BESIII Collaboration), *Phys. Rev. D* **92**, 072012 (2015).
- [51] $\mathcal{B}_{K_1 \rightarrow K^- \pi^+ \pi^-} = \frac{1}{3} \times \mathcal{B}_{K_1 \rightarrow K \rho} + \frac{4}{9} \times \mathcal{B}_{K_1 \rightarrow K^* (892) \pi} + \frac{4}{9} \times 0.93 \times \mathcal{B}_{K_1 \rightarrow K_0^* (1430) \pi} + \mathcal{B}_{K_1 \rightarrow K^+ \omega} \times \mathcal{B}_{\omega \rightarrow \pi^+ \pi^-}$ where K_1 denotes $K_1(1270)^-$.
- [52] M. Ablikim *et al.* (BESIII Collaboration), *Chin. Phys. C* **44**, 040001 (2020).
- [53] A. Bondar *et al.* (Charm-Tau Factory Collaboration), *Yad. Fiz.* **76**, 1132 (2013).
- [54] Z. Zhou *et al.*, 7th International Particle Accelerator Conference (IPAC 2016), Busan, Korea (2016).
- [55] E. Kou *et al.* (Belle II Collaboration), *PTEP* **2019**, 123C01 (2019); **2020**, 029201(E) (2020).
- [56] R. Aaij *et al.* (LHCb Collaboration), arXiv:1808.08865.